www.icgst.com

Automatic Pulmonary Embolism Detection System

Hao-Hung Tsai, Chiun-Li Chin, Yung-Chih Cheng
Department of Applied Information Sciences of the Chung Shan Medical University, Taichung, Taiwan.
Department of medical imaging, Chung Shan Medical University Hospital, Taichung, Taiwan
cshe232@csh.org.tw, ernestli@mercury.csmu.edu.tw, isethehey@hotmail.com

Abstract
Pulmonary embolism (PE) is a blockage of the main artery of the lung or one of its branches by a substance that has travelled from elsewhere in the body through the bloodstream. Most of the traditional PE detection methods need to depend on the professional physician's judgment. Serious PE will lead to dead. Therefore, it is very important for diagnosis PE. In this paper, we develop an automatic pulmonary embolism detection system for relieving doctor's load. It is divided into five parts- preprocessing, finding pulmonary, vessel searching, vessel tracking and evaluation. The experiment results show our system has 83% precision rate in main vessel detection and 82.6% precision rate in branch vessel detection. Finally, our system can relieve doctor's load according to the result of questionnaire analysis.

Keywords: *CT, ACM, pulmonary embolism*

1. Introduction
Pulmonary arterial embolism is a common emergency in medical treatment. According to the statistic from European Society of Cardiology, there are 100,000 cases per year in France; there are 65,000 cases per year in England and Wales Borderlands, and there are at least 60,000 cases per year in Italy. If there has an accurate diagnosis and medical treatment opportunely, it effective decreases the death rate to 2% ~ 8%. The general detection types can be separated into four types which are D-miner, X-ray, nuclear medicine and computer tomography (CT) etc. The first type D-II (D-Dimer) is the preparatory method to detect the PE. The positive rate of PaO2 is 65.9%, PaCO2 is 53.1%, and the accurate rate of D-Dimer is 70%. Even the sensitive rate is high, the accurate rate is low. X-ray can show infiltration, atelectasis, diaphragmatic eventration and pleural effusion in image, especially in the diagnosis of Hamptom based on pleura and the pulmonary artery with Westermark expanded shows the great contributions. But it is inaccurate and also weak to find the position of the embolism. Nuclear medicine uses the behavior of the radioisotope. It offers accurately on diagnosis with many diseases and makes the treatment more efficacious. But the disadvantage of using nuclear medicine is spending time and there is a problem of registration. Hence, we use CT as the data source to accomplish our system. The purpose of the system we proposed is constructing a system which can provide a high accurate rate helping the doctor's detection, decreasing the workload of doctors and the error occurrence.

In general, the velocity flow of local blood vessels with embolism will lower than other normal region. If getting the pulmonary blood flow distribution in detail, we can estimate the location and the incidence of pulmonary embolism. Qanadi SD, Hajjam ME and Mesurolle B [1] uses CTA to analyze whether there are emboli in pulmonary artery and vessel or not. The sensitivity and the discrimination rate were 90% and 94%, respectively. Unfortunately CTA does not show the good accurate rate in branch vessel. Qanadi SD, Hajjam ME and Mesurolle B [2] discovers using lung scan and CTA to detect the pulmonary embolism, the correction rate was only 60%. Nicholas J. Screaton and Harvey O. Coxson [3] indicate that the low sensitivity reason can divide into two parts. The first reason is that there are a large number of branch of vessel and the volumes are too slight to be observed. The doctor has to be very careful to diagnosis, and it may make the doctor too tired causing mistakes. Subsequently, every Computed Tomography Angiography (CTA) image can replace the actual data of lung about 2mm or 5mm. It may cause shifted phenomenon by breathing or heart beating. The shifted image makes the area which has lower CT value look like embolism in the branch. Hence, it will increase the error rate of detection embolism.

U. Joseph Schoeph and Nicolaus Holzknecht [4] proposes that it needed to be improved with CTA analysis to diagnose the embolism in branch vessel. According to statistical analysis, the normal perfusion and reduced perfusion of the region where exist embolism could be distinguished with CTA image after injecting the contrast medium [5]. We use the high or low CT value to determine the perfusion with single image or a sequence images. Wildberger and other researchers [6-8] use the image after injecting the contrast medium to observe the difference between the changes of CT value of lung area. It can reflect the difference of perfusion. Users can observe the unusual

area easily. At the same time, there were many computer science scholars develop an automatic algorithm to detect the location of pulmonary embolism [9-13]. They use a lot of image processing technology and artificial intelligence technique such as finding the outline and using neural networks, but the results of their accuracy and precision is not good enough.

Before performing the detection of pulmonary embolism, we need to find out the location of lung region in CTA image. There are some methods to segment each area in image with image processing, such as [14-15]. In addition, there are other methods to find the position of lung by using the features of lung or some symptoms. Park W., Hoffman E.A. and Sonka M [16] use the features of bronchial distributions. Blechschmidt R.A., Werthschutzky R and Lorcher U [17] use the features of emphysema. Brown M.S., McNitt-Gray M.F., Mankovich N.J., Goldin J.G., Hiller J., Wilson L.S. and Aberie D.R. [18] uses the fluid air in lung as the pulmonary feature. Dajnowiex, M., Alirezaie, J. and Yongbum Lee, Takeshi Hara, Hiroshi Fujita, Shigeki Itoh and Takeo Ishigaki [19-20] uses pulmonary tuberculum as the feature to find out the position of lung. Besides the above methods which use the features of lung to perform segmentation, some researches, such as [21-23], combine the threshold value of gray image with morphology operators to segment lung area, in which Shojaii, R. Alirezaie and J. Babyn, P. [23] uses the optimal threshold value obtained by automatic calculation to reduce the noise of background and keeping the biggest two areas. In our medical image database, some images have the problem of two lung images superimposition. In order to solve this problem, the calculation has to strengthening. U.J. Schoepf, N. Holzknecht, T.K. Helmberger, et al. [24] uses dynamic programming method to solve the problem of superimposed image. The others studies combined other technologies with knowledge to make the lung region to be separated. For example [16][18], it employs the information of logical structure and provides a powerful segmentation technique. But its shortcoming is high computational complexity. Methods mentioned above simply use the technology of image processing and experiences to get the result for solving the problem. But they donate guarantee a high accuracy, and also do not have a fixed steps to implement.

Subsequently, we discover that the contrast enhancement of local image can help to find the problem area. U.J. Schoepf, N. Holzknecht, T.K. Helmberger, et al [25] proves that using the contrast enhancement of CTA image with vessel part can help the medical diagnosis. C. Zhou, et al. [26] use computer-aided detection (CAD) method to find out the suspected pulmonary embolisms in the image. In visualization, E.A. Chiang, et al. [27] use Maximum Intensity Projection (MIP) method surrounding the heart to search the vessel. It can highlight the higher pixel value region such as the lung image and used it to detect the embolism position. Therefore, it is proper to detect the pulmonary embolism. A.P. Kiraly, D.P. Naidich, and C.L. Novak [28] proposes that the spin projection can segment vascular tree for improving the sensitivity in a few numbers of images. In addition, E. Pichon, C.L. Novak, A.P. Kiraly, D.P. Naidich, A.P. Kiraly, C.L. Novak, D.P. Naidich and Szeliski, R., and Tonnesen, D. and Terzopoilos D. [29-31] use the material within the vessel to determine the color of the vessel surface in 3D visual aspect. It provides observing all of the blood vessel quickly. These methods we mention above need to perform vessel tracking with 3D navigation method. But 3D navigation in image processing will reduce the efficiency of the system. A.P. Kiraly, D. P. Naidich and C. L. Novak [32-33] propose building the hierarchy tree method. It can raise efficiency of the vessel tracking. Besides, Henri Bouma, Jeroen J. Sonnemans, Anna Vilanova and Frans A. Gerritsen [34] use varied features of embolism such as intensity, shape and size and the location to detect whether there exists embolism in pulmonary artery or not.

According to the above literature review, we discover that_several CAD systems for PE have been proposed, but their evaluations have some problems. Firstly, their methods are complicated. Secondly, they use a lot of the range of CT values to remove unnecessary part in the CTA image according to professional doctor's knowledge. Finally, they do not have to process branch vessel in the lung area. For solving these problems, we propose an automatic pulmonary detection system and hope that our system can relieve doctor's fatigue.

The following sections describe details of the proposed method. In section 2, that is our methodologies, we will introduce our proposed detection flowchart and describe each processing procedure in detail. Section 3, it will show the experimental results. And section 4, we will make a conclusion and purpose the research topics in the future.

2. Methodologies

First, for observing the state of blood stream in lung, we inject contrast medium into lung. The contrast medium will follow the blood stream and distributes around every vessels in the lung. The lung area which injects contrast medium has higher CT value and looks brighter. The yellow circle area in the Fig. 1 shows the location of embolism. Because blood cannot pass through the embolism area, the contrast medium also cannot pass through it. Hence there does not have the effect of contrast medium, the CT value of embolism is lower than around area where passes through blood with contrast medium. The area which has pulmonary embolism in CTA image shows anomalous dark.

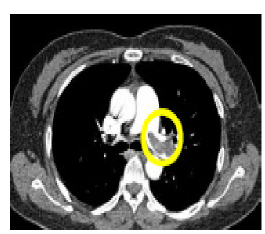

Figure 1 The CTA image with pulmonary embolism

Subsequently, we start to perform the pulmonary embolism detection task. Figure 2 shows the processing procedure of our proposed method. It is divided into four parts: the pre-processing, finding pulmonary, vessel searching and tracking, and using template matching method to evaluate the results between doctor and our system. We will introduce each processing step in detailed.

2.1 Pre-processing

The thickness of slice image we used is 1mm. It lets us observing the change of vessel clearly. But, the image has the noise if the thickness of slice image is too thin. The purpose of pre-processing is to obtain an image which can be analyzed. Therefore, we use a smoothing filter to reduce the noise on the original image. The filter uses a 3 × 3 mask to achieve. This mask performs convolution operator with original image from the top of left to bottom of right of the image. The value of central point will be replaced by the mean of the sum of another 8 points. Therefore, we obtain an image which was removed noise.

2.2 Finding Pulmonary Location

Next, we have to separate lung area standing alone from background area in the image. Here, we use Active Contour Model (ACM), which is proposed by Michael Kass, Andrew Witkin and Demetri Terzopoulos [35] to obtain the lung area in CTA image. ACM uses the contour points around the target pulmonary convergence method to get the target image contour.

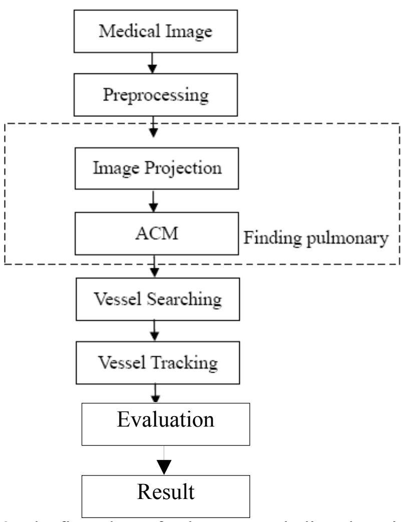

Fig. 2: The flow chart of pulmonary embolism detection

The advantage of using ACM is that it can achieve the goal of finding pulmonary image location automatically. Therefore, we have to set control points around the pulmonary before using ACM. We use image projection method to get those contour points around the target. These control points use B-spline Curve to associate an original contour.

The CT value of body fat is between bone and air. Therefore, when setting the contour points of the target, we can use this feature and combine with the projection on X and Y axis to achieve this task. Figure 3 and Figure 4 show the result of projection on X and Y axis, respectively. We project on X axis and Y axis respectively to get the center of valley. We get the center point of pulmonary in the image with intersection point obtained by the intersecting of center position of X and Y axis.

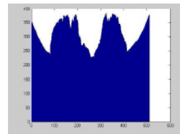

Figure 3 The projection image on X axis

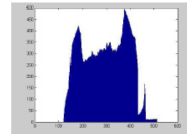

Figure 4 The projection image on Y axis

Here (a,b) is the center point, and a is the valley between two obvious peaks on the projection of X axis and b is the valley between two obvious peaks on the projection of Y axis. Using difference on the projection of X axis can find two huge peaks. The radius r is calculated by the distance on the first point (a_1,b_1) of the first huge peak and the end point (a_2,b_2) of the second huge peak. Hence, based on the characteristic of ACM, we set the contour points around the image of lung. And, the radius is the farther distance calculated from the center point (a,b) to (a_1,b_1) and (a_2,b_2). The expression equation is as the following.

$$r = \arg\max\left(\sqrt{(a_1-a)^2+(b_1-b)^2}, \sqrt{(a_2-a)^2+(b_2-b)^2}\right) \qquad (1)$$

When getting a contour circle, we use the angle ϕ obtained by edge detection method to produce a new contour point. We can obtain a contour of fitting pulmonary image edge with iterative step. Figure 5 shows the original image, Fig. 6 shows the initial contour in the image, and Figure 7 shows the image obtained by executing ACM.

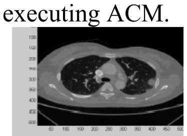

Figure 5 The original CTA

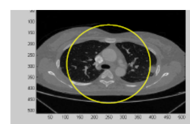

Figure 6 The initialization of ACM

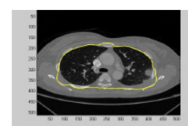

Figure 7 The image after using

2.3 Vessel Searching

Figure 8 shows the CTA image before injecting the contrast medium and Figure 9 shows the CTA image with contrast medium. Here, we divide processing step into two parts to perform. One is main vessel processing and the other is branch vessel processing. These two parts do not have the sequence of relationship about executing. The system integrates the results of two parts together and shows the analysis result. The main vessel contains pulmonary artery and aorta. The branch vessel contains other small vessels in lobe. Fig. 10 shows the flow chart of vessel searching.

Figure 8 The CTA image without injecting contrast medium

Figure 9 The CTA image after injecting contrast medium

Due to the blood with contrast medium does not flow to the same region at the best time with capture CTA image, the processing of branch vessel and main vessel are different. According to the professional doctor's suggestion, the optimal time to get the appropriate CTA image is the blood with contrast medium just passing through those main vessels.

At this moment, there is higher CT value at the main vessel. About the branch vessel part, the blood with contrast medium does not flow to here yet; the CT value of branch vessel is lower. According to the difference of mentioned above, the methods we used to search main vessel and branch vessel are different. We will introduce the detail from branch vessel searching to main vessel searching.

A. Branch vessel searching

First, we use the opening method of morphology of image processing to separate two region of lobe from background. It can help us to perform the following steps more easily. After getting the lobe image, we use histogram equalization method to enhance the contrast of lobe image for observing the detail in lobe.

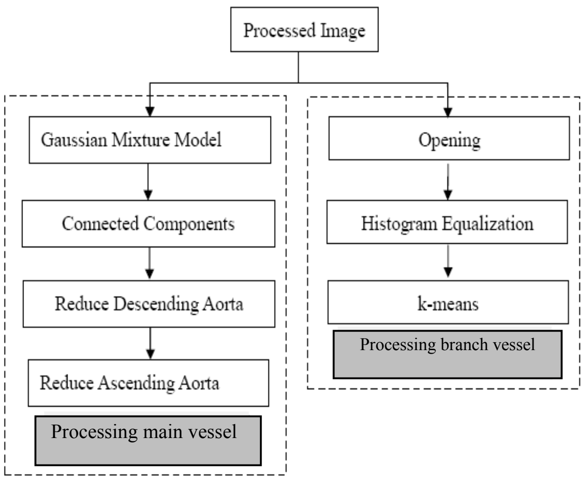

Figure 10: The flow chart of vessel searching

The contrast enhancement can be achieved with eq. 2. And the resulted image are shown on Fig. 11.

$$round(j) = \lambda \sum n_j \quad \text{where} \quad \lambda = \frac{L-1}{N} \qquad (2)$$

j represents gray value, $\sum n_j$ is the accumulating of j, L is the gray level of the image, and N is the total pixel number in the image.

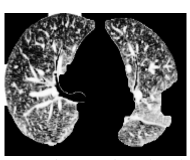

Figure 11 The lobe image after performing histogram equalization

When observing the Figure 11, we discover that the lobe region after performing histogram equalization not only enhances the vessel part clearly, but also enhances other detail parts. For only keeping vessel parts, we use k-means method to keep the more vessel parts for avoiding the interference the later steps. Because the observed data have been injected contrast medium, we will keep the cluster which has the cluster center of highest value. According to the professional doctor's decision and recognition, the data will be divided into 7 clusters. It can satisfy the requirement of detecting pulmonary embolism. Fig. 12 shows the result after performing k-means. Moreover, those areas after histogram equalization and k-means have very tiny parts for observing. These parts can not recognition by professional doctor. Therefore, we have combined connected components method to remove those very tiny areas in the image. Fig. 13 shows the resulted image after performing connected components.

B. Main vessel searching

As we know the pulmonary embolism will occur in the pulmonary vessel, we use Gaussain mixture model (GMM) to separate the main vessel and background. Figure 14 shows the resulted image after performing GMM to analyze the distribution of the pixel intensity in the image.

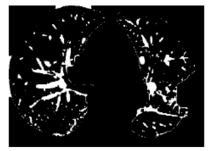

Figure 12 The vessel image in lobe after performing by k-means

Figure 13 The vessel image in lobe after performing connected components

Through by GMM processing, we get two clusters data parameters. These two parameters are the mean value and variance of each clustering, respectively. Because the images we used are injected contrast medium, we only keep the cluster which has the highest mean value in the result and segment vessel parts with other object in the background. Due to the bone intensity in the image shows the similar as normal vessel intensity, the bone area will also be kept after performing GMM. For keeping main vessel parts, the bone area and those small vessels around main vessel parts will treat as the noise which has to be removed. Hence, we combine connected components method again to remove those small areas in the image. Figure 15 shows the resulted image after performing connected components.

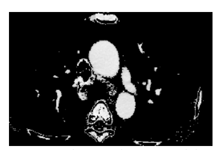

Figure 14 The main vessel image

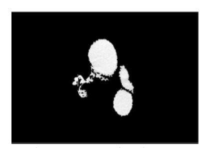

Figure 15 The image after performing

Subsequently, the image after performing GMM contains aorta (there are ascending aorta and descending aorta) with contrast medium. It will produce false contour in the aorta image when doctor captured the image. It will affect the precision rate for detecting pulmonary embolism. Therefore, we have to remove the false contours which are not belonging to pulmonary artery before performing vessel tracking. Figure 15 shows some objects, from up to bottom is ascending aorta, pulmonary artery and descending aorta. There are obvious gradient changes among all of them. Hence, according to the characteristic, we use image projection method to find the boundary value to achieve removing the aorta and keep the pulmonary artery goal. Figure 16 shows the flowchart of removing descending aorta. In the removing descending aorta part, after vertical projection, we obtain a histogram as Figure 17(a).

For raising the precision rate of the boundary, we use

the1-D smoothing filter to smooth the histogram for removing some noise, showing as Figure 17(b). Subsequently, we calculate the gradient of the histogram and smooth it in order to set the better boundary to remove the descending aorta. The result shows on Figure 17(c) and Figure 17(d). Figure 18 shows the image after removing descending aorta and backbone.

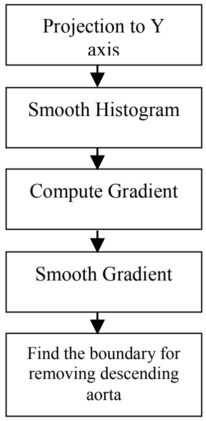

Fig. 16 The flow chart of removing descending aorta

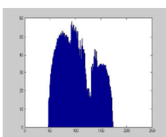

Fig. 17(a) the histogram of projection on Y axis

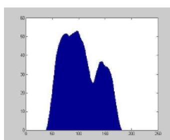

Fig. 17(b) Smoothing the Fig. 17(a)

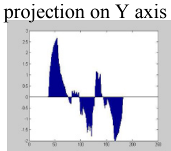

Figure 17(c) Computing the change of gradient

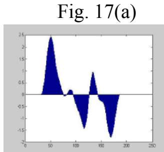

Figure 17(d) the smoothing of Fig. 17(c)

Figure 18 The image after removing

Figure 19 shows the algorithm of finding the boundary. The boundary value can separate the aorta and pulmonary artery. The input parameter array is the gradient array after smoothing.

```
Function boundary = count_boundary_dsc(array)
for j = R to 2
    value = array[j] * array[j-1];
    if value < 0
        boundary = j;
        break;
    end
end
```

Figure 19 The algorithm for finding the boundary

R is the position of starting searching. The position of R will change according to the different target. Assume W is the length of the gradient array, it is also the width of Y axis of the image. Due to the goal in here is removing the descending aorta, the calculation of starting searching position is $R=(7\times W)/10$. At the big change of gradient, the forward value and the backward are in different quadrants. Therefore, the values in different quadrants are multiplied to get the result which is lower than zero as the characteristic. The characteristic can find the boundary value. Then, we use the image shown on Figure 18 to perform removing ascending aorta. Fig. 22 shows the flow chart of removing ascending aorta. Our method makes the own mask of each image. The mask can remove the ascending aorta in the image. In the removing ascending aorta part, we need to perform twice boundary computation, one is on Y axis and the other is on X axis. Figure 20 and Figure 21 show the algorithm of removing ascending aorta. First, we use Equation 3 to perform projection on Y axis and use Equation 4 to perform smoothing on histogram. Then we use Equation 5 to find the boundary. The result shows on Figure 23. Subsequently, we use Figure 23 to perform projection on X axis, and then perform as above steps to smooth the histogram and calculate the boundary. The result shows on Figure 24.

$$Vproj(y)=\sum_{x=1}^{m} Ip(x,y)$$
$$\text{where } y=1,2,\ldots,n \quad (3)$$
$$Ip(x,y)=0 \quad \text{if} \quad I(x,y)=0$$
$$Ip(x,y)=1 \quad \text{if} \quad I(x,y)\neq 0$$

$$Smooth\_Vproj(y)=\frac{1}{p+1}\sum_{i=y-\frac{p}{2}}^{y+\frac{p}{2}} Vproj(i), \quad (4)$$
$$\text{where } y=(p/2)+1\ldots n-(p/2)$$

$$G(y)=(smooth\_Vproj[y+1]-smooth\_Vproj[y-1])/2,$$
$$\text{where } y=2,..,n-1$$
$$G(y)=smooth\_Vproj[y+1]-smooth\_Vproj[y], \quad (5)$$
$$\text{where } y=1$$
$$G(y)=smooth\_Vproj[y]-smooth\_Vproj[y-1]$$
$$\text{where } y=n$$

```
Function boundary = count_boundary_asc1(array)
for j = R to W-1
    value = array[j] * array[j+1];
    if value < 0
        boundary = j;
        break;
    end
end
```

Figure 20 The algorithm for finding the boundary on Y axis

The definition of $R=(3\times W)/8$, which represents the starting searching position, is the same as $C=H/2$ in the Fig. 20 and Fig. 21. And it will not be fixed according to the different target. The W is the length of gradient array, it is also the width on Y axis in the image. Here H is the length of the array, it is also the width on X axis in the image. Finally, we use the result of Fig. 24 as a mask to perform XOR operation with the corresponding position of original image. That will achieve the goal of removing ascending aorta. The result shows on Figure 25.

2.4 Vessel Tracking

In vessel tracking, we use the vessel distribution chart of pathology as the vessel skeleton chart. The vessel skeleton chart uses to track the alignment of the main

vessel.

```
Function boundary = count_boundary_asc2(array)
for j = C to H-1
    value = array[j] * array[j+1];
    if value < 0
        boundary = j;
        break;
    end
end
```

Figure 21 The algorithm for finding the boundary on X axis

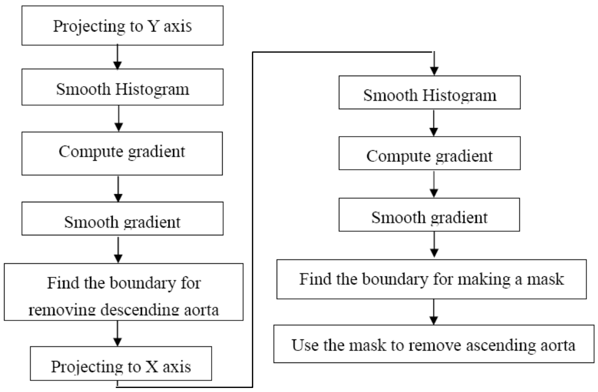

Figure 22: The flow chart for removing ascending aorta

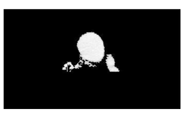

Fig. 23 The first result of performing finding boundary

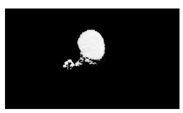

Fig. 24 The second result of performing finding boundary

Fig. 25 The image after removing ascending aorta

Due to the thickness of slices we used is 1mm, we can use such the details from slices to observe the change and build the vessel skeleton chart. After a series of background removing and backbone and aorta removing, there is pulmonary artery in the image. We know that the pulmonary embolism exists in pulmonary artery, so we perform pulmonary artery tracking and pulmonary embolism detection on the current image. In order to track becoming easier, we perform a preprocessing step before tracking pulmonary artery. Fig. 26 shows the flow chart of preprocessing for tracking pulmonary artery.

According to the doctor explanation, the pulmonary artery will grow into "人" shape in 2D CTA image. In this part, we perform projecting on X axis and find the bigger change in gradient of the image. For letting tracking pulmonary easily and faster, we divide the pulmonary artery into two parts. Figure 27 shows the result image after projecting and dividing. Figure 27(a) shows the image which is removed background noise, backbone and aorta removing. Figure 27(b) shows the left side of pulmonary artery and Figure 27(c) shows the right side of pulmonary artery.

Then, we use the thinning method of image processing to find the skeleton of the image after dividing. Here we will introduce the thinning method. Let a object as O, and its boundary is B. If there is a pixel t, e_1 and e_2 which t is in the object O and e_1, e_2 belong to boundary B.

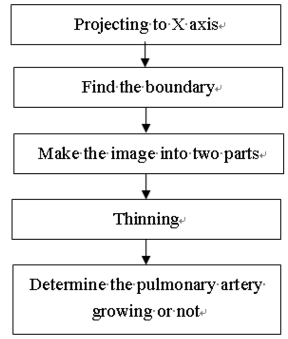

Figure 26 The preprocessing flow chart of pulmonary artery tracking

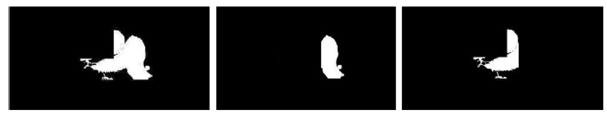

(a) (b) (c)

Figure 27 The pulmonary artery image. (a) Before performing projection and segmentation; (b) After performing projection and segmentation of the left pulmonary artery image; (c) After performing projection and segmentation of the right pulmonary artery image

If all of them can satisfy the distance function d as eq. 6, t can be regarded as the element of the skeleton of the object O.

$$d(t,e_1) = d(t,e_2) \qquad (6)$$

Here $d(t,e_i)$, $1 \le i \le 2$ represents the distance between t and e_i. In the part of distance function, we can get the different skeleton according to the different distance function. Here we use is Euclidean distance function to get the skeleton of pulmonary artery. The result shows on Figure 28. The black line represents the skeleton.

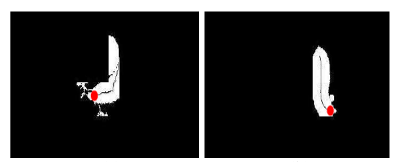

(a) (b)

Figure 28 The image contains pulmonary artery and its skeleton. (a) The skeleton of left pulmonary artery；(b) The skeleton of right pulmonary artery

Finally, we use the skeleton of pulmonary artery to track the pulmonary artery in the image whether the image has normal growing or not. Figure 29 shows the flow chart of pulmonary artery tracking. When getting the skeleton of pulmonary artery; meanwhile, we can obtain the endpoints of each skeleton. In Figure 28, the red point is the endpoint of skeleton. According to the image we used is a sequence 2D image, the image in time T and time $T+1$ will not have big changed. Hence, we use endpoints as the foundation to perform pulmonary artery tracking. Before tracking pulmonary artery, we will check a record file which records the position of endpoints.

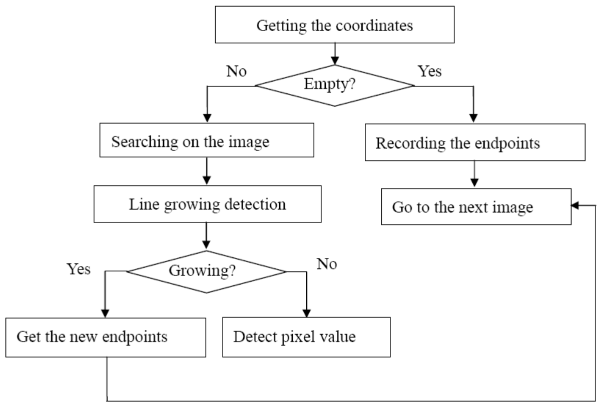

Figure 29 The flow chart for tracking pulmonary artery

If there does not have the endpoint records of forward image, we will record the endpoint of the current image to terminate tracking pulmonary artery and proceed processing for the next time image continually. On the contrary, if there is the endpoint information, then use this position to collate with the same position of the current image and detect the skeleton in the region whether it grows or not. If the skeleton grows, the system records the newest endpoint and detects whether it has the embolism characteristic in the new growing path. Otherwise, the system also detects the surrounding area of endpoint to understand whether it exist the feature of embolism or not.

Finally, according to the professional doctor's explanation, the CT value of embolism will not be variation change with different person. There is a characteristic about the CT value of embolism; that is, it has a fixed range. From the experiment, the CT value range of embolism is from 1050 ~ 1100 HU. We use the CT number range of embolism to be feature for detecting embolism in main and branch vessel.

2.5 Evalution

Here, we use the template matching method to achieve precision computing. The professional doctor will select the embolism places in the image to produce the grown truth image for all of the images. These grown truth images will be regarded as template images. The produced image of our system will be regarded as comparison image. The comparison image will compare with the ground truth image. And then, according to the comparison result, the precision rate will be calculated. The matching we used adopts blob-by-blob method to proceed. And then, we use the result of the output to take as the system performance.

3. Conclusion

A. The introduction of data set

The instrument to get the image is GE Fast Helcal CT. The data set we used all contain pulmonary embolism. The image is represented by 12 bits. The range of CT value of the image is from -2048 to 2048. We adjust the range of CT value into all of the positive values. Hence, the range will become from zero to 4095. The CTA image data is 2D CTA image data. The slices of the image is 1mm, the resolution of the image is 512×512. Each data set contains $250 \sim 280$ images, deducting those images without pulmonary artery; the real number of images is about $30 \sim 50$

B. Experimental results

Herein, we will divide the result into two parts to explain. First, we use twenty questionnaires to obtain doctor's operation suggestion. Next, through by the professional doctor's knowledge and suggestion, we adjust the system parameter. For example, the parameter of disk size of closing operator sets 2 and the execution time sets 1, we can get the better result. Figure 30 shows the CTA image with pulmonary embolism. Additionally, the branch vessels in lobe are hard to observe. The doctor also inconveniences to detect embolism on those branch vessels. But, our method can detect the pulmonary embolism in the branch vessel. Figure 31 shows the result.

Here, we enumerate some experimental results, the left images in the Figure 32 and Figure 33 are grown truth images and the right images are our experimental images. Fig. 32 shows the successful cased and Fig. 33 shows the failure cases. The red circles in the grown truth images are embolisms which are selected by the professional doctor. The white rectangles in the system images are embolisms which are selected by our system.

In the Figure 32, our system detects the embolisms position correctly. But in the Figure 33, some human tissues may cause this kind of error. For example, there are two embolisms in the pulmonary artery in the upper images o Figure 33. Because the first embolism does not stick the pulmonary artery entirely, our system loses the information of the first embolism; the bottom image shows the soft tissue in the intermediate pulmonary artery. As the experiment results, there are similar CT value of soft tissue, fat and embolism, our system will produce the error on these kinds of images.

Subsequently, we use TPR (or sensitivity), FNR and Precision (p) index to present recognition result. When the TRP and p value are higher and FNR value is lower, the system is better. Table 2 shows the performance of our system with using the CTA images from 16 patients to detect the embolism in the pulmonary artery. The average precision rate is about 0.83. From the above table, our system shows the lower TPR value but higher FNR value. That is because this experiment only uses pulmonary artery tracking to detect the embolism. If the pulmonary artery is in the growing stage and grows to the embolism not yet, our system cannot perform embolism detection. Table 3 shows the performance of our system in the branch vessel detection. The average precision rate is about 0.826.

Finally, we found some doctors to use our system. We use questionary method to get doctor's opinions. From the result of questionary analysis, we discover that there are 90% doctors to be willing used our system.

In this paper, we propose an automatic pulmonary embolism detection system. We will divide the problem into two parts to discuss. One is the main vessel processing. The other is branch vessel processing. They have different processing method. From experiment result, we discover that our proposed method has 83% successful rate and can find the pulmonary embolism in

branch vessel. The successful rate in branch vessel detection is 82.6%. The system will efficient relieve doctor's loading.

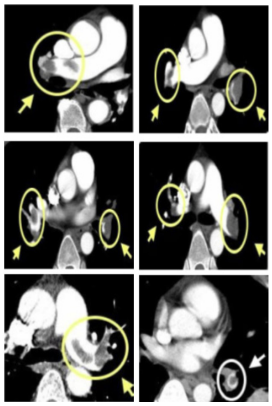

Figure 30 The images with pulmonary embolism.

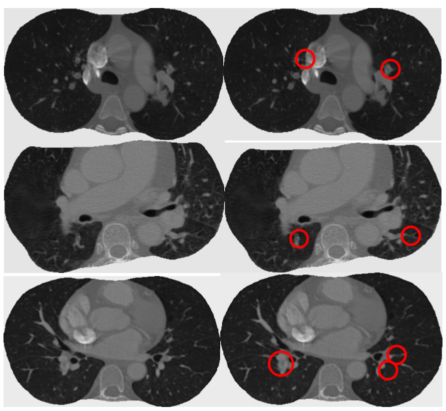

Figure 31 The left images are original image and the right images are the image with pulmonary embolism in branch vessel.

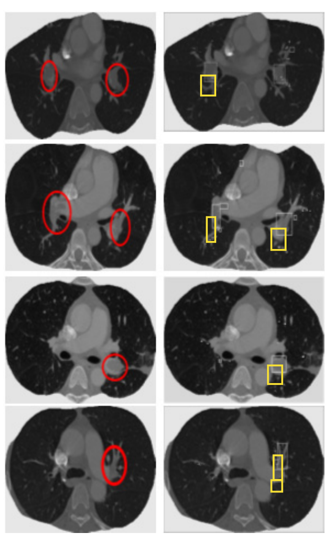

Figure 32 The experiment results (Successful cases)

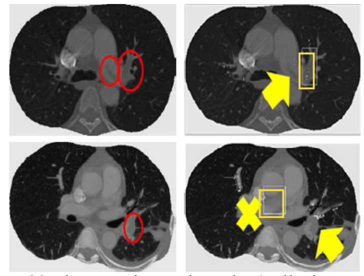

Figure 33 The experimental results (Fallacious cases)

Table 2: The performance of our system in main vessel

Data set No.	*TPR*	*FNR*	*p*
A patient	0.5	0.5	0.75
B patient	0.58	0.42	0.82
C patient	0.53	0.47	0.79
D patient	0.6	0.4	0.84
E patient	0.57	0.43	0.82
F patient	0.47	0.53	0.78
G patient	0.55	0.45	0.83
H patient	0.66	0.34	0.85
I patient	0.7	0.3	0.9
J patient	0.68	0.32	0.87
K patient	0.63	0.37	0.86
L patient	0.56	0.43	0.82
M patient	0.52	0.48	0.8
N patient	0.71	0.29	0.91
O patient	0.5	0.5	0.75
P patient	0.6	0.4	0.84

Table 3: The performance of our system in branch vessel

Data set No.	*TPR*	*FNR*	*p*
A patient	0.55	0.45	0.80
B patient	0.60	0.40	0.84
C patient	0.47	0.53	0.75
D patient	0.62	0.38	0.86
E patient	0.40	0.60	0.72
F patient	0.48	0.52	0.76
G patient	0.56	0.44	0.83
H patient	0.66	0.34	0.85
I patient	0.70	0.30	0.9
J patient	0.68	0.32	0.87
K patient	0.63	0.37	0.86
L patient	0.58	0.42	0.83
M patient	0.52	0.48	0.81
N patient	0.75	0.25	0.95
O patient	0.51	0.49	0.77
P patient	0.61	0.39	0.81

4. Acknowledgements

The authors would like to thank the department of medical imaging, Chung Shan Medical University Hospital, Taichung, Taiwan, for medical image providing and help.

5. References

[1] Bouma, H. Sonnemans, J.J. Vilanova, A. Gerritsen, "Automatic detection of Pulmonary embolism in CTA images," IEEE Transaction on medical imaging, Vol. 28, pp. 1223-1230, 2009.
[2] Michiels JJ, Hoogsteden H and Pattynama PM, "Non-invasive diagnosis of pulmonary embolism," Acta Chir Belg, Vol. 1, pp. 26-34, 2005.
[3] P. Stein, S.E. Fowler, L.R. Goodman e.a, " Multidetector computed tomography for acute pulmonary embolism," New Engl. J. Med., Vol. 354, pp. 2317-2327, 2006.
[4] U. Joseph Schoeph and Nicolaus Holzknecht, "Subsegmental pulmonary emboli: improved detection with thin-collimation multi-detector row spiral CT," Radiology, pp. 483-490, 2002.
[5] Reinhard Groell and Karl H. Peichel, "Computed tomography densitometry of the lung: a method to assess perfusion defects in acute pulmonary embolism," European Journal of Radiology, Vol. 32, pp. 192-196, 1999.
[6] Joachim E. Wildberger and U. Joseph Schoepf, "Approaches to CT perfusion imaging in pulmonary embolism," Seminar Roentgenol, Vol. 40, pp. 64-73, 2005.
[7] Peter Herzog and Joachim E. Wildberger, "CT perfusion imaging of the lung in pulmonary embolism," Academic Radiology, Vol. 10, pp. 1132-1146, 2003.
[8] Wildberger JE, Niethammer MU and Klotz E, "Multi-slice CT for visualization of pulmonary embolism using perfusion weighted color maps," Fortschr Rontgenstr, Vol. 173, pp. 289-294, 2001.
[9] Simon J. Scurrell, "Automatic detection of pulmonary embolism using computation intelligence," A dissertation of university of the Witwatersrand, October 2006.
[10] Schoepf UJ and Costello P, "CT angiography for diagnosis of pulmonary embolism: state of the art," Radiology, Vol. 230, pp. 329-337, 2004.
[11] A. Frigyesi, "An automated method for the detection of pulmonary embolism in V/Q scans," Medical Image Analysis, Vol. 7, No. 7, pp. 341-349, 2003.
[12] R. Damper and I. Middleton, "Segmentation of magnetic resonance images using a combination of neural networks and active contour models," Medical Engineering & Physics, Vol. 26, No. 1, pp. 71-86, January 2003.
[13] Rafael C. Gonzalez and Richard E. Woods, "Digital Image Processing," Addison-Wesley Publishing Company, 1993.
[14] Margarida Silveira and Jorge Marques, "Automatic segmentation of the lungs using multiple active contours and outlier model," IEEE Engineering in Medicine and Biology Society Annual International Conference, pp. 3122-3125, 2006.
[15] D. Xu, J. Lee, D.S. Raicu, J.D. Furst and D.Channin, "Texture Classification of Normal Tissues in Computed Tomography," The 2005 Annual Meeting of the Society for Computer Applications in Radiology, Orlando, Florida, June 2-5, 2005.
[16] Park W., Hoffman E.A. and Sonka M, "Segmentation of intrathoracic airway trees: a fuzzy logic approach," IEEE Transaction on Medical Imaging, vol. 17, No. 8, pp. 489-197, Aug. 1998.
[17] Blechschmidt R.A., Werthschutzky R and Lorcher U, "Automated CT image evaluation of the lung: a morphology-based concept," IEEE Transactions on Medical Imaging, Vol. 20, No.5, pp. 434-442, 2001.
[18] Dajnowiex, M. and Alirezaie, J., "Computer simulation for segmentation of lung nodules in CT images," IEEE International Conference on Systems Man and Cybernetics, Vol. 5, pp. 4491-4496, 2004.
[19] Yongbum Lee, Takeshi Hara, Hiroshi Fujita, Shigeki Itoh and Takeo Ishigaki, "Automated detection of pulmonary nodules in helical CT images based on an improved template-matching technique," IEEE Transactions on Medical Imaging, Vol. 20, No. 7, pp. 595-604 , 2001.
[20] Augusto Silva, Jose S. Silva, Beatriz S. Santos and Carlos Ferreira, "Fast Pulmonary Contour Extraction in X-ray CT images: A Methodology and Quality Assessment," Medical Imaging 2001: Physiology and Function from Multidimensional Images, Vol. 4321, pp. 216-224, 2001.
[21] Hu s., Hoffman E. A., Reinhardt and J. M., "Automatic lung segmentation for accurate quantitation of volumetric X-ray CT images," IEEE Transactions on Medical Imaging, Vol. 20, No. 6, pp. 490-498 , 2001.
[22] Shojaii, R. Alirezaie and J. Babyn, P., "Automatic lung segmentation in CT images using Watershed Transform," IEEE International Conference on Image Processing, Vol. 2, pp. 1270-1273, 2005.
[23] U.J. Schoepf, N. Holzknecht, T.K. Helmberger, et al., "Subsegmental pulmonary emboli: improved detection with thin-collimation multi-detector row spiral CT," Radiology, Vol.2, pp. 483-490, 2002.
[24] Y. Masutani, H. MacMahon and K. Doi, "Computerized detection of pulmonary embolism in spiral CT angiography based on volumetric image analysis," IEEE Transactions on Medical Imaging, Vol. 21, Issue 12, pp. 1517-1523, 2002.
[25] C. Zhou, et al., "Computerized detection of pulmonary embolism in 3D computed tomographic (CT) images: vessel tracking and segmentation techniques," In Medical Imaging 2003: Image Processing. Proceedings of the SPIE, Vol. 5032, pp. 1613-1620, May 2003.
[26] E.A. Chiang, et al., "Detection of pulmonary embolism: comparion of paddlewheel and coronal CT reformations-initial experience," Radiology 228 (2), pp. 577-582, 2003.
[27] A.P. Kiraly, D.P. Naidich, and C.L. Novak, "Cartwheel projections of segmented pulmonary vasculature for the detection of pulmonary

embolism," Medical Imaging 2005:Image guided procedures, and display. Proceedings of SPIE - Int'l. Society for Optical Engineering, Vol. 5733, Part 1, pp. 69-78, 2005.
[28] E. Pichon, C.L. Novak, A.P. Kiraly and D.P. Naidich, "A novel method for pulmonary emboli visualization from high-resolution CT images," SPIE Medical Imaging, Vol. 5367, pp.161-170, 2004.
[29] A.P. Kiraly, C.L. Novak and D.P. Naidich, "A visualization-Based Method for Pulmonary Emboli Identification within High-Resolusion CT Images," European Congress of Radiology, 2005.
[30] A.P. Kiraly, "3D Image Analysis and Visualization of Tubular Structures," PhD thesis, The Pennsylvania State University, 2003.
[31] A.P. Kiraly, D. P. Naidich and C. L. Novak, "2D display of a 3D tree for pulmonary embolism detection," Computer-aided Radiology and Surgery - CARS 2005 - Proceedings of the 19th Int'l. Congress and Exhibition, Vol. 1281, pp. 1132-1136, 2005.
[32] Henri Bouma, Jeroen J. Sonnemans, Anna Vilanova and Frans A. Gerritsen, "Automatic Detection of Pulmonary Embolism in CTA Images," IEEE Transactions on Medical Imaging, Vol. 28, No. 8, August 2009.

Biographies

Hao-Hung Tsai was born in Hsinchu, Taiwan in 1973. He received his medical doctor from the Faculty of Post-Baccalaureate Medicine Department, Kaohsiung Medical University, Kaohsiung, Taiwan, in 2003. He is a visiting staff of the department of medical imaging, Chung Shan Medical University Hospital, Taichung, Taiwan from 2007 to now. His research interest is medical image of breast and chest.

Chiun-Li Chin was born in Taipei, Taiwan in 1975. He received his Ph.D degree in the electrical and control engineering from National Chiao Tung University, Hsinchu, Taiwan, in 2006, and his M.S. degree in electric engineering from Chung Hua University in 2000. He is an Assistant Professor of the Department of Applied Information Sciences of the Chung Shan Medical University, Taichung, Taiwan. From Jan. 2008 to Jan. 2010, His research interests include adaptive signal processing, image and video recognition, medical image processing, and embedded system.

Kun-Ching Wang was born in Kaohsiung, Taiwan in 1976. He received his Ph.D degree in the electrical and control engineering from National Chiao Tung University, Hsinchu, Taiwan, in 2005, and his M.S. degree in electric engineering from Feng Chia University in 2000. He is an Assistant Professor of the Department of Information Technology & Communication of the Shin Chien University, Kaohsiung, Taiwan. From Jan. 2007 to Jan. 2008, He was a Design Engineer of Digital Signal Processing Tech. Dept., Industrial Technology Research Institute, Chutung, Hsinchu, Taiwan. His research interests include adaptive signal processing, speech recognition, speech enhancement, and digital IC design.

Yung-Chih Cheng was born in Nantou, Taiwan in 1986. She received her Master degree in the Application of Information Sciences from Chung Shan Medical University, Taichung, Taiwan, in 2010. She is a Ph. D. student of the Department of Computer Science and Information Engineering of National Cheng Kung University, Tainan, Taiwan. From July 2008, her research interest is medical image processing.